



OPEN

A label-free fluorescent probe for Hg^{2+} and biothiols based on graphene oxide and Ru-complex

SUBJECT AREAS:

FLUORESCENT PROBES

BIOANALYTICAL CHEMISTRY

Linlin Wang, Tianming Yao, Shuo Shi, Yanlin Cao & Wenliang Sun

Department of Chemistry, Tongji University, Shanghai 200092, China.

Received
3 January 2014Accepted
27 May 2014Published
17 June 2014

Correspondence and requests for materials should be addressed to T.M.Y. (tmyao@tongji.edu.cn) or S.S. (shishuo@tongji.edu.cn)

A novel, selective and sensitive switch-on fluorescent sensor for Hg^{2+} and switch-off fluorescent probe for biothiols was developed by using $[\text{Ru}(\text{bpy})_2(\text{pip})]^{2+}$ as the signal reporter and graphene oxide (GO) as the quencher. Due to the affinity of GO towards single-stranded DNA (ss-DNA) and $[\text{Ru}(\text{bpy})_2(\text{pip})]^{2+}$, the three components assembled, resulting in fluorescence quenching. Upon addition of Hg^{2+} , a double-stranded DNA (ds-DNA) via T- Hg^{2+} -T base pairs was formed, and $[\text{Ru}(\text{bpy})_2(\text{pip})]^{2+}$ intercalated into the newly formed ds-DNA. Then, $[\text{Ru}(\text{bpy})_2(\text{pip})]^{2+}$ and ds-DNA were removed from the surface of GO, resulting in the restoration of fluorescence. Subsequently, upon addition of biothiols, Hg^{2+} was released from ds-DNA, due to the higher affinity of Hg^{2+} to the sulfur atoms of biothiols, which could induce ds-DNA unwinding to form ss-DNA. Then ss-DNA and $[\text{Ru}(\text{bpy})_2(\text{pip})]^{2+}$ were adsorbed on the surface of GO, the fluorescence of $[\text{Ru}(\text{bpy})_2(\text{pip})]^{2+}$ was quenched again. Therefore, the changes in emission intensity of $[\text{Ru}(\text{bpy})_2(\text{pip})]^{2+}$ directly correlated to the amount of detection target (Hg^{2+} or biothiols) in solution. The assay exhibited high sensitivity and selectivity, with the limits of detection for Hg^{2+} , cysteine (Cys) and glutathione (GSH) to be 2.34 nM, 6.20 nM and 4.60 nM, respectively.

H g^{2+} is one of the most toxic heavy metals. Even at low concentration, it is a threat to the human health and environment due to its ability of accumulation in ecological system¹. Mercury poisoning induces a wide variety of serious human diseases, including brain damage², kidney failure, and various cognition and motion disorders³. Therefore, the interest in developing rapid, specific, and cost-effective tools to detect Hg^{2+} is steadily growing. Much effort has been made to develop the Hg^{2+} sensors, including electrochemical sensors^{4,5}, colorimetric sensors^{6,7}, and fluorimetric sensors^{8–14}. Among them, functional nucleic acid sensors have recently received considerable attention, based on the fact that thymine base pairs can selectively capture Hg^{2+} to form T- Hg^{2+} -T base pairs¹⁵. However, Most of the existing fluorescent probes rely on label fluorophores and some of them require expensive labeling procedures. Furthermore, some of them are signal-off sensors, which can be troubled by false positives.

Biological thiols such as cysteine (Cys), homocysteine (Hcy), and glutathione (GSH) play essential roles in human physiology¹⁶. Abnormal levels of biothiols are connected with many diseases^{17,18}. It's of great interest to develop efficient methods for detection and quantification of biothiols. Up to date, lots of strategies such as liquid chromatography¹⁹, capillary electrophoresis²⁰, voltammetry²¹ and flow injection²², have been designed to detect biothiols. However, these methods generally require expensive instrument and tedious preparation protocols that limit the scope of their application. In the past few years, optical assays based on synthetic colorimetric and fluorescent probes have received increasing attention due to the simplicity, sensitivity and efficiency²³.

In this paper, we propose a turn on and label-free fluorescent probe for Hg^{2+} with high sensitivity and selectivity. The simple sensing platform for Hg^{2+} detection is based on a T-rich ss-DNA and the fluorescence resonance energy transfer (FRET) between graphene oxide (GO) and the Ruthenium complex, $[\text{Ru}(\text{bpy})_2(\text{pip})]^{2+}$ (Probe 1: T-rich ss-DNA, GO and $[\text{Ru}(\text{bpy})_2(\text{pip})]^{2+}$, P1) (Fig. 1). Initially, $[\text{Ru}(\text{bpy})_2(\text{pip})]^{2+}$ shows strong fluorescence in Tris-HCl buffer (pH = 7.0) at room temperature. $[\text{Ru}(\text{bpy})_2(\text{pip})]^{2+}$ can be adsorbed on the surface of GO to form a charge-transfer complex (GO-Ru) via π - π interactions and electrostatic interactions, and fluorescence of $[\text{Ru}(\text{bpy})_2(\text{pip})]^{2+}$ can thus be quenched by GO. The GO surface can also adsorb another component, i.e., T-rich ss-DNA, via π - π stacking, whenever T-rich ss-DNA is introduced into the probe system. In presence of Hg^{2+} in solution, T-rich ss-DNA will coordinate with Hg^{2+} through thymine base (T) due to its higher affinity to Hg^{2+} , be detached from the GO surface. Two T-rich ss-DNAs will be coupled via T- Hg^{2+} -T base pairs to give ds-DNA. Subsequently, $[\text{Ru}(\text{bpy})_2(\text{pip})]^{2+}$ can be removed from the GO surface, and intercalates into

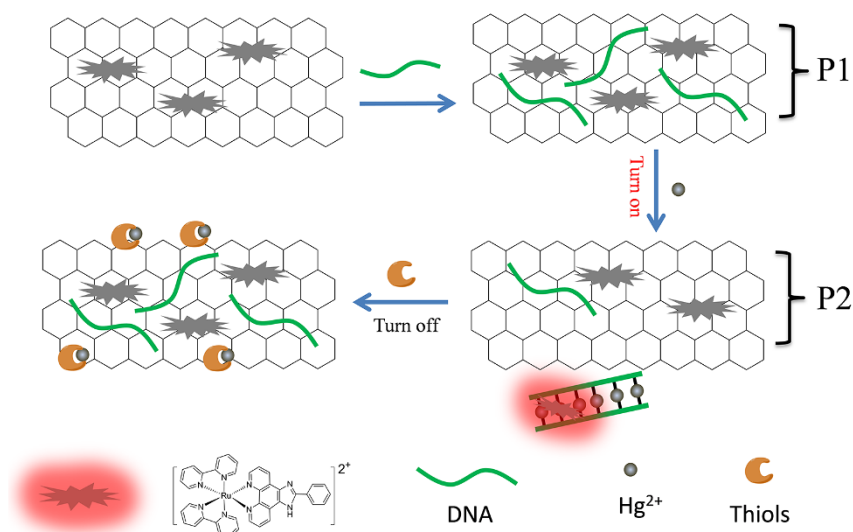


Figure 1 | Schematic description of Hg^{2+} and thiols detection mechanism based on GO-Ru complex and T-rich ss-DNA.

the newly formed ds-DNA, resulting in the restoration of fluorescence. Accordingly, the restoration in fluorescent intensity of $[\text{Ru}(\text{bpy})_2(\text{pip})]^{2+}$ directly correlate to the amount of detection target (Hg^{2+}) in solution.

On the other hand, the S-donor atoms originated from biothiols exhibits higher affinity to Hg^{2+} . Hence, upon addition of biothiols into the above GO-Ru- DNA/ Hg^{2+} system, Hg^{2+} can be released from ds-DNA coupled by T- Hg^{2+} -T base pairs, and ds-DNA unwind to give ss-DNA. Then ss-DNA and $[\text{Ru}(\text{bpy})_2(\text{pip})]^{2+}$ can be adsorbed on the surface of GO, and the fluorescence of $[\text{Ru}(\text{bpy})_2(\text{pip})]^{2+}$ is quenched again. (Probe 2: GO, T-rich DNA, $[\text{Ru}(\text{bpy})_2(\text{pip})]^{2+}$ and Hg^{2+} , P2) (Fig. 1). Herein, a highly selective fluorescence method for the detection of biothiols based on T-rich DNA, $[\text{Ru}(\text{bpy})_2(\text{pip})]^{2+}$, Hg^{2+} and GO has thus been introduced.

Results

GO was synthesized from graphite powder based on the Hummer's method²⁴. The TEM images of GO (a) and GO-Ru hybrid (b) were given in Fig. S2. It was noted that the GO surface was rough with a significant number of wrinkles. However, the surface of GO-Ru hybrid became more smooth, due to homogeneous adsorption of $[\text{Ru}(\text{bpy})_2(\text{pip})]^{2+}$ on the surface of GO. The UV/Vis spectra of $[\text{Ru}(\text{bpy})_2(\text{pip})]^{2+}$, GO and GO-Ru hybrid were shown in Fig. S3. The absorption peaks of both Ru-complex and GO were slightly broadened and red shifted ($\Delta\lambda = 3 \sim 10$ nm), during the binding process of $[\text{Ru}(\text{bpy})_2(\text{pip})]^{2+}$ on GO surface to give GO-Ru hybrid. This is indicative of strong π - π stacking, hydrogen bonding and electrostatic interactions between GO and Ru-complex. Furthermore, the Raman spectra (Fig. S4) and FTIR spectra (Fig. S5) also provided direct evidences for the interaction between Ru complex and GO, and all these data were in good agreement with literatures²⁵⁻²⁷.

The fluorescence intensity of $[\text{Ru}(\text{bpy})_2(\text{pip})]^{2+}$ (2.0 μM) decreased rapidly when GO was added into the solution (Fig. S6 A). The fluorescence of the $[\text{Ru}(\text{bpy})_2(\text{pip})]^{2+}$ was quenched almost completely by GO, due to the strong interaction between $[\text{Ru}(\text{bpy})_2(\text{pip})]^{2+}$ and GO, and the quenching efficiency was estimated to be 85% when the concentration of GO was 5.0 $\mu\text{g}/\text{mL}$. Hence, in this paper, $[\text{Ru}(\text{bpy})_2(\text{pip})]^{2+}$ was accordingly used as the signal-reporter, and its final concentrations were kept to be 2.0 μM , while a final concentration of GO as the quencher was 5.0 $\mu\text{g}/\text{mL}$. It was noticed that the quenching efficiency of GO became a little lower, with the presence of T-rich ss-DNA in $[\text{Ru}(\text{bpy})_2(\text{pip})]^{2+}$ solution (Fig. S6 B), indicating a slight interaction

between $[\text{Ru}(\text{bpy})_2(\text{pip})]^{2+}$ and T-rich ss-DNA, although this interaction was much weaker than that between $[\text{Ru}(\text{bpy})_2(\text{pip})]^{2+}$ and GO. Certainly this interaction may have impact on the detection, however, it can be deduced by background calibration.

For a successful design of Hg^{2+} assay, an optimal selection of T-rich ss-DNA is pivotal. In this work, three oligonucleotides, with different base sequence and length (from short to longer), were firstly selected and tested. They are: T₁₀ (5'-GGGT TTTT TTTT TCCC-3'), T₂₁ (5'-TTTT TTTT TTTT TTTT TTTT T-3'), and T₃₀ (5'-TTTT TTTT TTTT TTTT TTTT TTTT TTTT TT-3'). As illustrated in Fig. 2, with the addition of Hg^{2+} into solution, T₃₀ showed the highest fluorescence restoration, while T₁₀ showed the lowest fluorescence restoration. On the other hand, it was interestingly noticed that T₁₀ showed a better sensitivity for Hg^{2+} , as demonstrated in Fig. S7 and Fig. S8. In addition to the length of the ss-DNA, a possible factor to account for the sensitivity could be the different affinities of nucleobases towards Hg^{2+} , the relative binding energy was reported

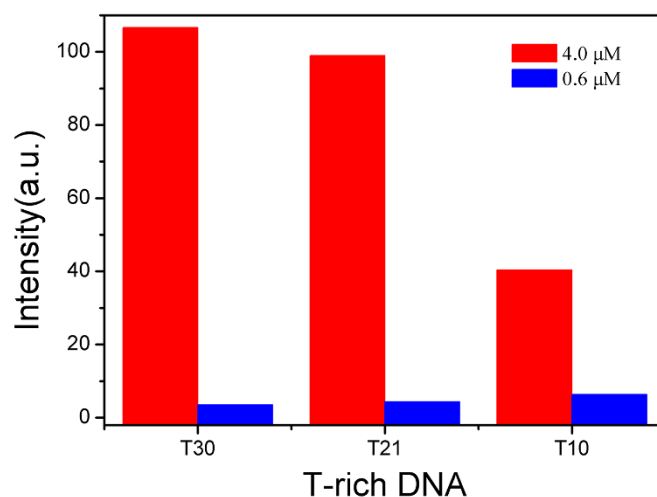


Figure 2 | The fluorescence responses of different T-rich DNA at the concentrations of Hg^{2+} of 4.0 μM (■) and 0.6 μM (■). T10: T₁₀ + Hg^{2+} + GO + $[\text{Ru}(\text{bpy})_2(\text{pip})]^{2+}$; T21: T₂₁ + Hg^{2+} + GO + $[\text{Ru}(\text{bpy})_2(\text{pip})]^{2+}$; T30: T₃₀ + Hg^{2+} + GO + $[\text{Ru}(\text{bpy})_2(\text{pip})]^{2+}$; The concentrations of T-rich DNA and $[\text{Ru}(\text{bpy})_2(\text{pip})]^{2+}$ were 3.0 μM and 2.0 μM , respectively. The concentration of GO was 5.0 $\mu\text{g}/\text{mL}$. The excitation and emission wavelengths were 455 nm and 605 nm, respectively.

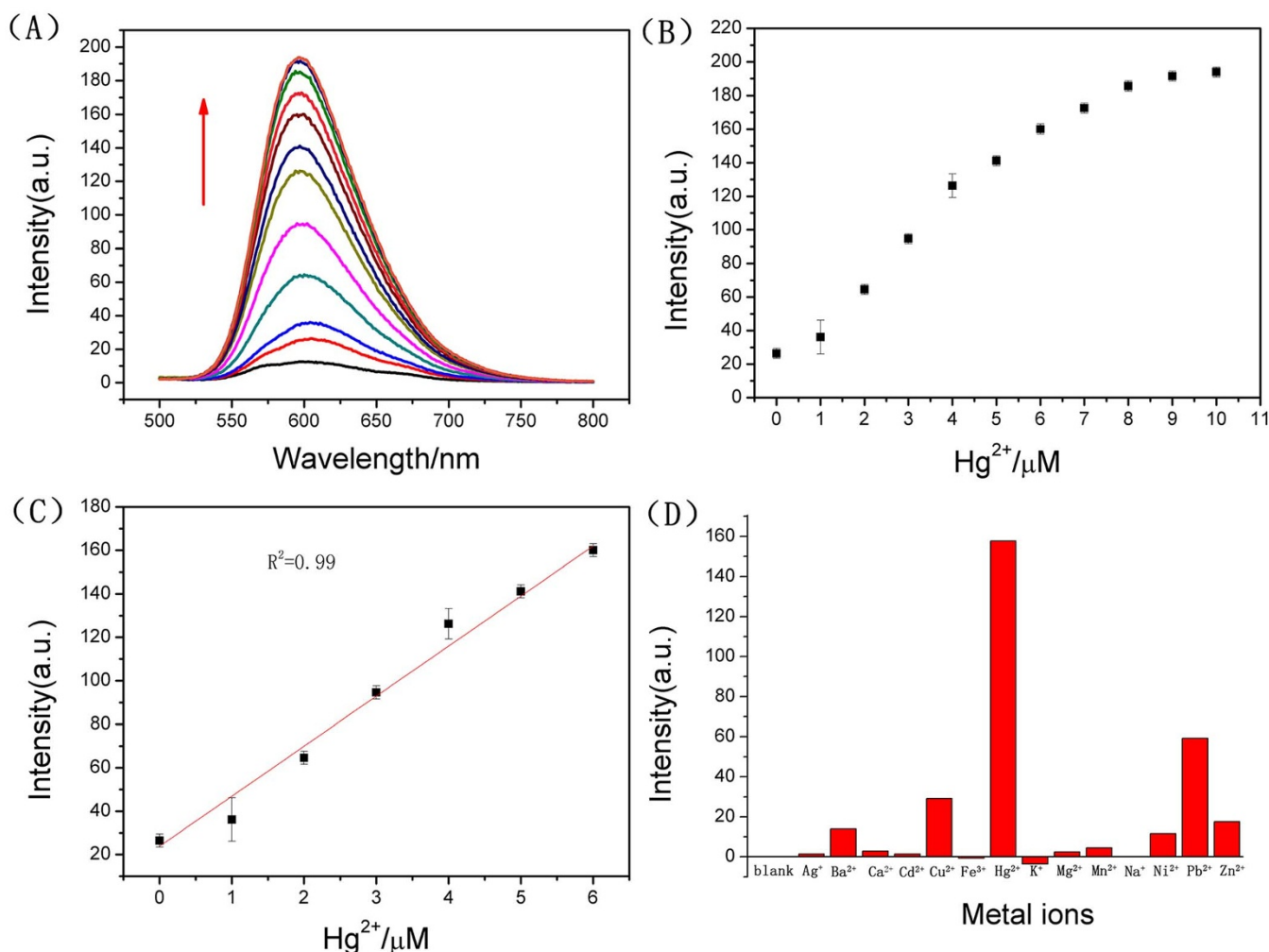


Figure 3 | (A) Fluorescence spectra of the GO-Ru-T₂₁ system (P1) (GO = 5.0 μg/mL, Ru = 2.0 μM, T₂₁ = 3.0 μM.) at different concentrations of Hg²⁺ (from bottom to top: 0, 1.0, 2.0, 3.0, 4.0, 5.0, 6.0, 7.0, 8.0, 9.0, and 10.0 μM (the bottom black line was the fluorescence spectrum of GO-Ru complex)) in 10 mM Tris-HCl buffer (pH = 7.0) at room temperature. (B) Fluorescence intensity of P1 against the concentrations of Hg²⁺. (C) The linear relationship of the fluorescence intensity of the P1 against the concentrations (0–6 μM) of Hg²⁺. (D) Selectivity of the fluorescent probe to Hg²⁺ against different metal ions. The concentration of Hg²⁺ was 6.0 μM while the other metal ions were 10.0 μM. The excitation and emission wavelengths were 455 nm and 605 nm, respectively.

to be in the series G > A > C > T in aqueous medium²⁸. Therefore, as a compromise for efficiency, selectivity, even as well as cost, T₂₁ was finally selected by us for constructing fluorescent probe for Hg²⁺.

To clarify the different interactions that may exist within the detection system, a systematic investigation was carried out, as shown in Fig. S9. The fluorescence intensity of [Ru(bpy)₂(pip)]²⁺ had no obvious change, in the presence of Hg²⁺ ions, indicating no obvious interaction existed between [Ru(bpy)₂(pip)]²⁺ and Hg²⁺. The fluorescence intensity of [Ru(bpy)₂(pip)]²⁺ increased only about 42%, when [Ru(bpy)₂(pip)]²⁺ mixed with T-rich ss-DNA (T₂₁), indicating a weak interaction existed between [Ru(bpy)₂(pip)]²⁺ and T₂₁. However, the fluorescence intensity of [Ru(bpy)₂(pip)]²⁺ increased up to 152%, if both Hg²⁺ ions and T-rich ss-DNA (T₂₁) were present in the system. In this case, Hg²⁺ coordinated with the thymine on T₂₁, and the single-strand DNA (T₂₁) was coupled through T-Hg²⁺-T coordination bonds to give double-strand DNA. Then, [Ru(bpy)₂(pip)]²⁺ could intercalate between the T-Hg²⁺-T ds-DNA base pairs, resulting in a transferring of the ruthenium complex [Ru(bpy)₂(pip)]²⁺ from dark state to bright state²⁹.

The response curve of the turn-on sensor for Hg²⁺ is displayed in Fig. 3A. A linear relationship (R² = 0.99) (Fig. 3C) towards Hg²⁺ is

observed in the range of 0.0–6.0 μM. The limit of detection for Hg²⁺ was calculated to be 2.34 nM, based on 3σ/slope (σ, standard deviation of the blank samples).

The selectivity of the approach for Hg²⁺ is evaluated by comparing its response to Hg²⁺ and that to other metal ions (Ag⁺, Ba²⁺, Ca²⁺, Cd²⁺, Co²⁺, Cu²⁺, K⁺, Li⁺, Mg²⁺, Mn²⁺, Na⁺, Ni²⁺, Zn²⁺, Pb²⁺ and Sn²⁺). As shown in Fig. 3D, it was noticed that the fluorescent probe (P1) designed by us had excellent selectivity for Hg²⁺ (6.0 μM), over other metal ions even at a much higher concentration (10.0 μM). An anti-jamming capability testing¹⁰ for the fluorescent probe (P1) was also conducted. In Fig. S10, the results indicated again that the designed sensor had excellent anti-jamming capability and outstanding selectivity.

It is worth noting that the GO-Ru-T₂₁ fluorescent probe (P1) can be expediently combined with mercury ion (Hg²⁺, at a constant concentration) to give another sensor system, GO-Ru-T₂₁/Hg²⁺ fluorescent probe (P2) to detect biothiols. Interestingly it brings another important application for us, based on a competition mechanism previously described^{30,31}. Cysteine (Cys) or Glutathione (GSH) can effectively sequester Hg²⁺ by the formation of the strong S-Hg²⁺ bond. Therefore, this probe can be functioned as a fluorescence switch-off probe for biothiols such as Cys and GSH.

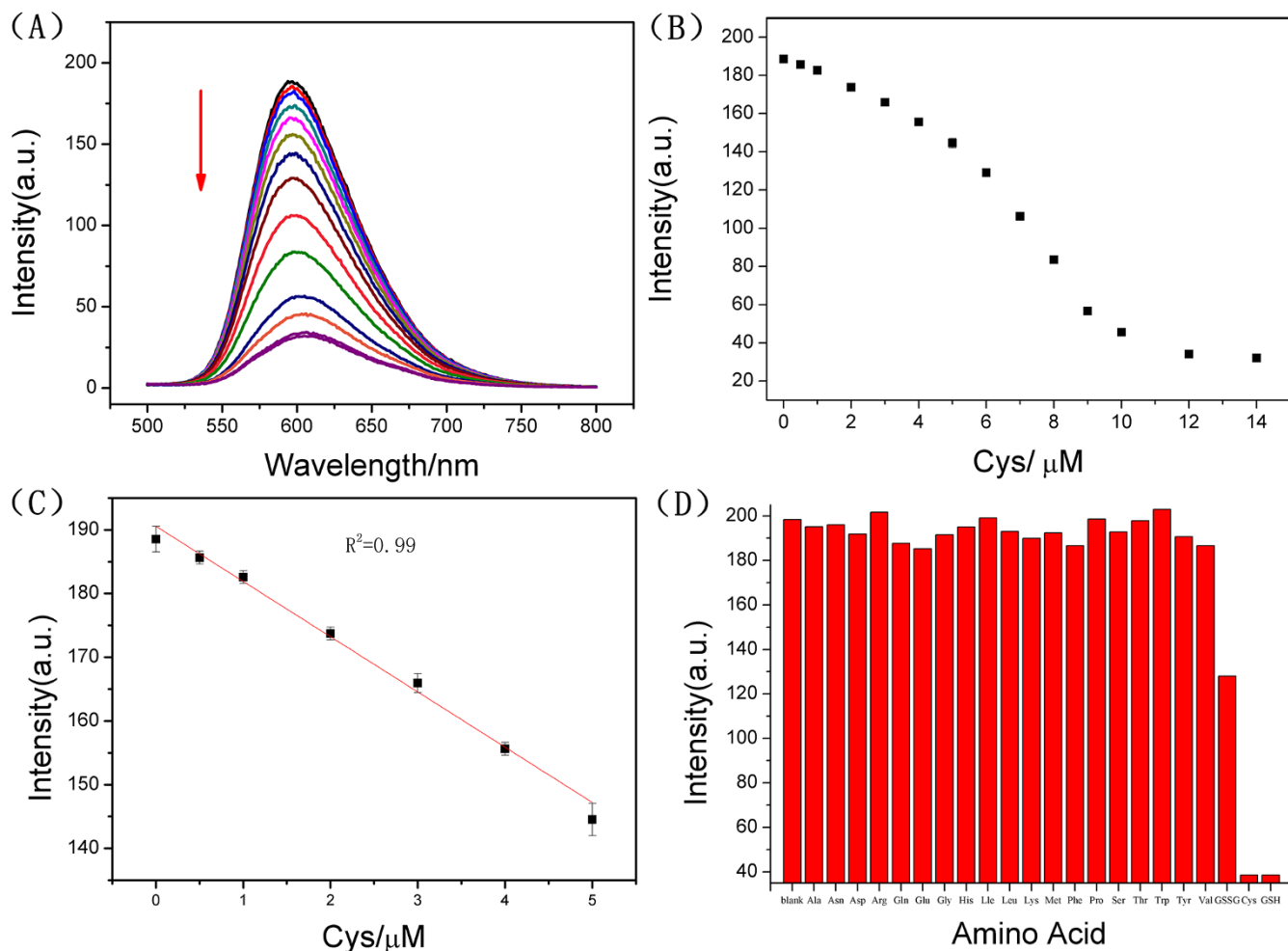


Figure 4 | (A) Fluorescence spectra of the GO-Ru-T₂₁/Hg²⁺ system (P2) (GO = 5.0 μg/mL, Ru = 2.0 μM, T₂₁ = 3.0 μM, [Hg²⁺] = 9.0 μM) in the presence of increasing concentrations of Cys (0, 0.5, 1.0, 2.0, 3.0, 4.0, 5.0, 6.0, 8.0, 10.0, 12.0 and 14.0 μM). (B) Fluorescence intensity of P2 against the concentrations of Cys. (C) The linear relationship of the fluorescence intensity of the P2 against the concentrations (0–5 μM) of Cys. (D) Selectivity of the fluorescent probe to Cys/GSH against different amino acids. The relative fluorescence intensity of fluorescent probe in the presence 10 μM Cys, GSH, GSSG and 100 μM other various amino acids. The excitation and emission wavelengths were 455 nm and 605 nm, respectively.

To maximize the efficiency of the detection system, we firstly incubated the T₂₁ with Hg²⁺ for 30 mins to ensure the full formation of the T-Hg²⁺-T ds-DNA, then GO-Ru hybrid was added and incubated for 30 mins again, prior to addition of Cys. With Cys concentration increasing, a gradual decrease in the fluorescence intensity at 605 nm was observed, with a linear relationship ($R^2 = 0.99$) in the range from 0.0–5.0 μM, as shown in Fig. 4A, B and C. The limit of detection for Cys was calculated to be 6.20 nM (based on 3 s/slope).

Furthermore, the GO-Ru-T₂₁/Hg²⁺ sensor system (P2) could also be applied to the detection of GSH under the same experimental conditions. With GSH concentration increasing, a gradual decrease in the fluorescence intensity at 605 nm was observed, with a linear relationship ($R^2 = 0.99$) in the range from 0.0–5.0 μM, and a limit of detection of 4.60 nM (Fig. S11). Generally the sensor system displayed the same response to Cys or GSH, because either Cys or GSH molecule contains one thiol group. However, it was interestingly to find that the sensor system could discriminate glutathione (GSH) in different oxidation states. As shown in Fig. S12, with the presence of oxidized Glutathione (GSSG), the fluorescence decrease could hardly be observed. A possible explanation for this phenomenon should be that the disulfide bond in GSSG couldn't provide donor atom for the coordination with Hg²⁺.

To clarify the response mechanism of the sensor system, we carried out an experiment, to test whether the fluorescence change was caused by the direct interaction of Cys/GSH with [Ru(bpy)₂(pip)]²⁺. The result was given Fig. S13. It was found that the fluorescence intensity did not change if Cys or GSH was added into 2.0 μM [Ru(bpy)₂(pip)]²⁺ solution, even the concentration of Cys or GSH became as high as 20 μM. This result ruled out the possibility that the fluorescence response resulted from the direct interaction between Cys/GSH and [Ru(bpy)₂(pip)]²⁺. Therefore, the fluorescence decrease of the sensor system really depended on the removal of Hg²⁺ from T-Hg²⁺-T ds-DNA, by the coordination of Cys or GSH with Hg²⁺.

To investigate the detection platform's selectivity for biothiols, the fluorescence responses to the other common amino acids (Ala, Asn, Asp, Arg, Gln, Glu, Gly, His, Ile, Leu, Lys, Met, Phe, Pro, Ser, Thr, Trp, Tyr, Val) were also recorded, at the amino acid concentration of 100 μM, 10 times higher than the detecting target - biothiol. In Fig. 4D, It was clearly observed that no significant fluorescence decrease appeared with the addition of other common amino acids, except for Cys and/or GSH. An anti-jamming capability testing for the fluorescent probe (P2) was also carried out. In Fig. S14, the results indicated that the designed sensor had excellent selectivity, as well as a satisfied anti-jamming capability for detection of Cys/GSH against other common amino acids.



Discussion

Graphene oxide (GO), with aromatic domains and carboxyl groups, is a remarkable nanomaterial for sensing applications³². The interesting and important example is that GO can differentiate various DNA structures such as ss-DNA, ds-DNA and stem-loops. Even though both ss-DNA and GO are negatively charged, ss-DNA can still be adsorbed on the surface of GO in buffers containing a high concentration of salt to screen electrostatic repulsion³³. The attractive forces between DNA and GO include π - π stacking, hydrophobic interaction, hydrogen bonding, and van der Waals forces³⁴. Compared to ss-DNA, the affinity between ds-DNA/quadruplexes and GO is much weaker^{35–37}. Adsorbed ss-DNA can be desorbed by adding its complementary DNA (cDNA) or some other targets to form a duplex/G-quadruplexes^{35,36,38}. On the other hand, GO can be used as a good quencher, since fluorophores adsorbed on GO are effectively quenched by electron transfer or energy transfer²⁵. These interesting properties of GO have been exploited to develop a highly sensitive fluorescent sensor^{39,40}.

[Ru(bpy)₂(pip)]²⁺ (bpy = 2,2'-bipyridine; pip = 2-phenylimidazo[4,5-f][1,10] phenanthroline) has prominent DNA-binding properties for DNA^{41–44}. It is ideally suitable for application as sensitive non-covalent probes for physical properties of DNA. Compared with conventional organic dyes, [Ru(bpy)₂(pip)]²⁺ possesses a variety of advantages, such as large Stokes shifts, coordinatively saturated, abundant optical properties, and inert to substitution. Furthermore, owing to its π -electron-rich framework and positive charge, [Ru(bpy)₂(pip)]²⁺ could interact with GO by π - π interactions, hydrogen bonding and electrostatic interactions^{27,45,46}. The tapping mode AFM image of the GO indicated that the average thickness of GO sheets is \sim 1.1 nm (Fig. S1, above), and the average size of GO is above 500 nm (Fig. S1). However, the mean thickness of Ru-GO hybrid was determined to be \sim 1.4 nm (Fig. S1, below). The significant increase in thickness of Ru-GO hybrid probably resulted from the covering of [Ru(bpy)₂(pip)]²⁺ molecules on the surface of GO sheet via π - π interactions. This data might provided a direct proof that [Ru(bpy)₂(pip)]²⁺ could be adsorbed on the surface of GO.

In summary, in this paper, we have successfully integrated the versatile functions of Graphene oxide (GO), with the distinct features of ruthenium complex [Ru(bpy)₂(pip)]²⁺ and T-rich ss-DNA, to develop a label-free, selective detection strategy for Hg²⁺ and biothiols. The turn-on fluorescent sensor for Hg²⁺ is based on the competitive binding of [Ru(bpy)₂(pip)]²⁺ with GO, or with ds-DNA. The ds-DNA is only given with the presence of Hg²⁺, by coupling T-rich ss-DNA via T-Hg²⁺-T base pairs. Thus this turn-on step can be applied to sensing mercury ion. Subsequently, this sensor system can also be utilized to detect biothiols (Cys or GSH). The higher affinity of the sulfur atoms of biothiols to Hg²⁺ can induce ds-DNA formed by T-Hg²⁺-T based pair unwinding to give ss-DNA. Then [Ru(bpy)₂(pip)]²⁺ is released from ds-DNA, and adsorbed again on the surface of GO, leading to the quenching of [Ru(bpy)₂(pip)]²⁺ fluorescence. The assay exhibited high selectivity and sensitivity, with the limits of detection for Hg²⁺, cysteine (Cys) and glutathione (GSH) to be 2.34 nM, 6.20 nM and 4.60 nM, respectively. We expect that this strategy may offer a new approach for developing low cost and sensitive sensors in biological and environmental applications.

Methods

Preparation of GO. GO was synthesized from graphite powder based on the Hummer's method²⁴. Graphite powder of spectrographic grade was purchased from Sinopharm Chemical Reagent Co. Ltd. (China).

Synthesis of [Ru(bpy)₂(pip)]²⁺. [Ru(bpy)₂(pip)]²⁺ was synthesized by the literature routes⁴¹.

Preparation of GO-Ru hybrid. 5.0 mL GO solution (100.0 μ g/mL) and 1.0 mL Ru(bpy)₂(pip)]²⁺ solution (200.0 μ M) were mixed in a 15.0 mL plastic centrifuge

tube, and diluted with 4.0 mL ultrapure water. Then the solution was sonicated at 20°C for 20 minutes in order to fully mixed and dispersed, to get GO-Ru hybrid. The final concentrations of [Ru(bpy)₂(pip)]²⁺ and GO were 20.0 μ M and 50.0 μ g/mL, respectively.

Preparation of DNA. Three purified T-rich oligonucleotides (T₁₀ (5'-GGGT-TTTT-TTTT- TCCC-3'); T₂₁ (5'-TTTT TTTT TTTT TTTT TTTT T-3'); T₃₀ (5'-TTTT TTTT TTTT TTTT TTTT TTTT TT-3')) were obtained from Sangon Biotechnology Co., Ltd (Shanghai, China). The stock solutions of oligonucleotides were prepared in 10 mM Tris-HCl buffer (pH = 7.0). The DNA solutions were heated at 90°C for 6 minutes to dissociate any intermolecular interaction, and gradually cooled to room temperature (25°C). Then, the DNA solutions were stored at 4°C before use. The stock solutions were diluted by Tris-HCl buffer (10 mM, pH 7.0) to required concentration prior to use. Lambda Bio 40 UV-vis Spectrophotometer (Perkin-Elmer, USA) was used to quantify the oligonucleotides, with the extinction coefficients (ϵ /M⁻¹cm⁻¹, at 260 nm) for each nucleotide: G = 11500, C = 7400, T = 8700.

Fluorescence response curve of Hg²⁺. T₂₁ (final concentration: 3.0 μ M) and different amount of Hg²⁺ (final concentration: 0, 1.0, 2.0, 3.0, 4.0, 5.0, 6.0, 7.0, 8.0, 9.0, and 10.0 μ M, respectively) was mixed and diluted with buffer (10 mM Tris-HCl buffer, pH = 7.0) to a final volume of 900 μ L, in a 1.5 mL plastic centrifuge tube, and incubated for 30 minutes to ensure full formation of the T-Hg²⁺-T ds-DNA. Then 100 μ L GO-Ru hybrid was added and incubated for another 30 minutes. The fluorescence spectra were recorded at room temperature on an F-7000 fluorescence spectrophotometer (Hitachi) with a quartz cell (1 cm). The excitation and emission wavelengths were 455 nm and 605 nm, respectively. Both excitation slit width and emission slit width were 10 nm.

Fluorescence response curve of Cys/GSH. T₂₁ (final concentration: 3.0 μ M) and Hg²⁺ (final concentration: 9.0 μ M) was mixed and diluted with buffer (10 mM Tris-HCl buffer, pH = 7.0) to a final volume of 800 μ L, in a 1.5 mL plastic centrifuge tube, and incubated for 30 minutes to ensure full formation of the T-Hg²⁺-T ds-DNA. Then 100 μ L GO-Ru hybrid was added and incubated for 30 minutes. Next, different amount of Cys or GSH was added to the solution to the final concentration of 0, 0.5, 1.0, 2.0, 3.0, 4.0, 5.0, 6.0, 8.0, 10.0, 12.0 and 14.0 μ M, respectively, and diluted with buffer (10 mM Tris-HCl buffer, pH = 7.0) to a final volume of 1.0 mL, incubated again for 10 minutes. The fluorescence spectra were recorded at room temperature on an F-7000 fluorescence spectrophotometer (Hitachi) with a quartz cell (1 cm). The excitation and emission wavelengths were 455 nm and 605 nm, respectively. Both excitation slit width and emission slit width were 10 nm.

- Eisler, R. Health Risks of Gold Miners: A Synoptic Review. *Environ. Geochem. Health* **25**, 325–345 (2003).
- Yang, D. J., Shi, S., Yao, T. M. & Ji, L. N. Cooperative folding of tau peptide by coordination of group IIB metal cations during heparin-induced aggregation. *Biometals* **25**, 361–372 (2012).
- Tchounwou, P. B., Ayensu, W. K., Ninashvili, N. & Sutton, D. Review: Environmental exposure to mercury and its toxicopathologic implications for public health. *Environ. Toxicol.* **18**, 149–175 (2003).
- Guo, L. Q., Yin, N., Nie, D. D., Fu, F. F. & Chen, G. N. An ultrasensitive electrochemical sensor for the mercuric ion via controlled assembly of SWCNTs. *Chem. Commun.* **47**, 10665–10667 (2011).
- Tang, C. X., Zhao, Y., He, X. W. & Yin, X. B. A "turn-on" electrochemiluminescent biosensor for detecting Hg²⁺ at femtomole level based on the intercalation of Ru(phen)₃²⁺ into ds-DNA. *Chem. Commun.* **46**, 9022–9024 (2010).
- Xie, W. Y., Huang, W. T., Zhang, J. R., Luo, H. Q. & Li, N. B. A triple-channel optical signal probe for Hg²⁺ detection based on acridine orange and aptamer-wrapped gold nanoparticles. *J. Mater. Chem.* **22**, 11479–11482 (2012).
- Kanayama, N., Takarada, T. & Maeda, M. Rapid naked-eye detection of mercury ions based on non-crosslinking aggregation of double-stranded DNA-carrying gold nanoparticles. *Chem. Commun.* **47**, 2077–2079 (2011).
- Wu, J.-S., Hwang, I.-C., Kim, K. S. & Kim, J. S. Rhodamine-Based Hg²⁺-Selective Chemodosimeter in Aqueous Solution: Fluorescent OFF–ON. *Org. Lett.* **9**, 907–910 (2007).
- Xie, J., Zheng, Y. & Ying, J. Y. Highly selective and ultrasensitive detection of Hg²⁺ based on fluorescence quenching of Au nanoclusters by Hg²⁺-Au⁺ interactions. *Chem. Commun.* **46**, 961–963 (2010).
- Huang, D. et al. Highly Sensitive Strategy for Hg²⁺ Detection in Environmental Water Samples Using Long Lifetime Fluorescence Quantum Dots and Gold Nanoparticles. *Environmental Science & Technology* **47**, 4392–4398 (2013).
- Zhu, G., Li, Y. & Zhang, C.-y. Simultaneous detection of mercury(II) and silver(I) ions with picomolar sensitivity. *Chem. Commun.* **50**, 572–574 (2014).
- Li, M., Zhou, X. J., Ding, W. Q., Guo, S. W. & Wu, N. Q. Fluorescent aptamer-functionalized graphene oxide biosensor for label-free detection of mercury(II). *Biosens. Bioelectron.* **41**, 889–893 (2013).
- Zhang, X. R., Li, Y., Su, H. R. & Zhang, S. S. Highly sensitive and selective detection of Hg²⁺ using mismatched DNA and a molecular light switch complex in aqueous solution. *Biosens. Bioelectron.* **25**, 1338–1343 (2010).



14. Zhu, Z. C., Xu, L., Zhou, X., Qin, J. G. & Yang, C. L. Designing label-free DNA sequences to achieve controllable turn-off/on fluorescence response for Hg²⁺ detection. *Chem. Commun.* **47**, 8010–8012 (2011).
15. Xu, H. F. *et al.* Molecular beacon, fluorescent sensor for detection of mercury II ion in aqueous solution. *Chem. Commun.* **47**, 12158–12160 (2011).
16. Zhang, S. Y., Ong, C. N. & Shen, H. M. Critical roles of intracellular thiols and calcium in parthenolide-induced apoptosis in human colorectal cancer cells. *Cancer Lett* **208**, 143–153 (2004).
17. Townsend, D. M., Tew, K. D. & Tapiero, H. The importance of glutathione in human disease. *Biomed. Pharmacother.* **57**, 145–155 (2003).
18. Dalton, T. P., Shertzer, H. G. & Puga, A. Regulation of gene expression by reactive oxygen. *Annu. Rev. Pharmacol. Toxicol.* **39**, 67–101 (1999).
19. Amarnath, K., Amarnath, V., Amarnath, K., Valentine, H. L. & Valentine, W. M. A specific HPLC-UV method for the determination of cysteine and related aminothiols in biological samples. *Talanta* **60**, 1229–1238 (2003).
20. Chen, G., Zhang, L. Y. & Wang, J. Miniaturized capillary electrophoresis system with a carbon nanotube microelectrode for rapid separation and detection of thiols. *Talanta* **64**, 1018–1023 (2004).
21. Ndamani, J. C., Bai, J., Qi, B. & Guo, L. P. Application of electrochemical properties of ordered mesoporous carbon to the determination of glutathione and cysteine. *Anal. Biochem.* **386**, 79–84 (2009).
22. Zhao, C., Zhang, J. C. & Song, J. F. Determination of L-Cysteine in Amino Acid Mixture and Human Urine by Flow-Injection Analysis with a Biamperometric Detector. *Anal. Biochem.* **297**, 170–176 (2001).
23. Jung, H. S., Chen, X. Q., Kim, J. S. & Yoon, J. Y. Recent progress in luminescent and colorimetric chemosensors for detection of thiols. *Chem. Soc. Rev.* (2013).
24. Hummers, W. S. & Offeman, R. E. Preparation of Graphitic Oxide. *J. Am. Chem. Soc.* **80**, 1339–1339 (1958).
25. Balapanuru, J. *et al.* A graphene oxide-organic dye ionic complex with DNA-sensing and optical-limiting properties. *Angew. Chem. Int. Ed.* **49**, 6549–6553 (2010).
26. Chandra, V. & Kim, K. S. Highly selective adsorption of Hg²⁺ by a polypyrrole-reduced graphene oxide composite. *Chem. Commun.* **47**, 3942–3944 (2011).
27. Li, H. *et al.* Interaction of Ru(phen)₃Cl₂ with graphene oxide and its application for DNA detection both in vitro and in vivo. *J. Mater. Chem. B* **1**, 4146–4151 (2013).
28. Varghese, N. *et al.* Binding of DNA nucleobases and nucleosides with graphene. *Chem. Phys. Chem.* **10**, 206–210 (2009).
29. Yao, J. L. *et al.* A naked-eye on-off-on molecular “light switch” based on a reversible “conformational switch” of G-quadruplex DNA. *Inorg. Chem.* **51**, 12591–12593 (2012).
30. Leung, K. H. *et al.* A luminescent G-quadruplex switch-on probe for the highly selective and tunable detection of cysteine and glutathione. *Chem. Commun.* **49**, 771–773 (2013).
31. Zhou, L., Lin, Y. H., Huang, Z. Z., Ren, J. S. & Qu, X. G. Carbon nanodots as fluorescence probes for rapid, sensitive, and label-free detection of Hg²⁺ and biothiols in complex matrices. *Chem. Commun.* **48**, 1147–1149 (2012).
32. Morales-Narváez, E. & Merkoçi, A. Graphene Oxide as an Optical Biosensing Platform. *Adv. Mater.* **24**, 3298–3308 (2012).
33. Liu, J. W. Adsorption of DNA onto gold nanoparticles and graphene oxide: surface science and applications. *Phys. Chem. Chem. Phys.* **14**, 10485–10496 (2012).
34. Zhao, X. C. Self-Assembly of DNA Segments on Graphene and Carbon Nanotube Arrays in Aqueous Solution: A Molecular Simulation Study. *J. Phys. Chem. C* **115**, 6181–6189 (2011).
35. Liu, X. Q., Wang, F. A., Aizen, R., Yehezkeli, O. & Willner, I. Graphene Oxide/Nucleic-Acid-Stabilized Silver Nanoclusters: Functional Hybrid Materials for Optical Aptamer Sensing and Multiplexed Analysis of Pathogenic DNAs. *J. Am. Chem. Soc.* **135**, 11832–11839 (2013).
36. Liu, B. W., Sun, Z. Y., Zhang, X. & Liu, J. W. Mechanisms of DNA sensing on graphene oxide. *Anal. Chem.* **85**, 7987–7993 (2013).
37. Huang, P. J. & Liu, J. W. Separation of Short Single- and Double-Stranded DNA Based on Their Adsorption Kinetics Difference on Graphene Oxide. *Nanomaterials* **3**, 221–228 (2013).
38. Xie, W. Y., Huang, W. T., Li, N. B. & Luo, H. Q. Design of a dual-output fluorescent DNA logic gate and detection of silver ions and cysteine based on graphene oxide. *Chem. Commun.* **48**, 82–84 (2012).
39. Wen, Y. Q. *et al.* A graphene-based fluorescent nanoprobe for silver(I) ions detection by using graphene oxide and a silver-specific oligonucleotide. *Chem. Commun.* **46**, 2596–2598 (2010).
40. Premkumar, T. & Geckeler, K. E. Graphene–DNA hybrid materials: Assembly, applications, and prospects. *Prog. Polym. Sci.* **37**, 515–529 (2012).
41. Wu, J. Z. *et al.* Bis(2,2′-bipyridine)ruthenium(II) complexes with imidazo[4,5-f][1,10]-phenanthroline or 2-phenylimidazo[4,5-f][1,10]phenanthroline. *J. Chem. Soc., Dalton Trans.* 1395–1402 (1997).
42. Shi, S. *et al.* Interaction of [Ru(bpy)₂(dppz)]²⁺ with human telomeric DNA: Preferential binding to G-quadruplexes over i-motif. *Biochimie* **92**, 370–377 (2010).
43. Sun, W. L., Yao, T. M. & Shi, S. A molecular light switch Ru complex and quantum dots for the label-free, aptamer-based detection of thrombin. *Analyst* **137**, 1550–1552 (2012).
44. Xiong, Y. & Ji, L. N. Synthesis, DNA-binding and DNA-mediated luminescence quenching of Ru(II) polypyridine complexes. *Coord. Chem. Rev.* **185–186**, 711–733 (1999).
45. Sun, W., Shi, S. & Yao, T. Graphene oxide-Ru complex for label-free assay of DNA sequence and potassium ions via fluorescence resonance energy transfer. *Anal. Methods* **3**, 2472–2474 (2011).
46. Yu, Y. *et al.* Synthesis of electrochemiluminescent graphene oxide functionalized with a ruthenium(II) complex and its use in the detection of tripropylamine. *Carbon* **50**, 2539–2545 (2012).

Acknowledgments

This work was supported by the National Natural Science Foundation of China (no. 81171646, no.31170776, and no. 20901060) and the Fundamental Research Funds for the Central Universities.

Author contributions

The work was conducted under the direction of T.M.Y. and S.S. All the experiments were performed by L.L.W. The paper was written by L.L.W., T.M.Y. and S.S. All authors reviewed the manuscript.

Additional information

Supplementary information accompanies this paper at <http://www.nature.com/scientificreports>

Competing financial interests: The authors declare no competing financial interests.

How to cite this article: Wang, L.L., Yao, T.M., Shi, S., Cao, Y.L. & Sun, W.L. A label-free fluorescent probe for Hg²⁺ and biothiols based on graphene oxide and Ru-complex. *Sci. Rep.* **4**, 5320; DOI:10.1038/srep05320 (2014).



This work is licensed under a Creative Commons Attribution-NonCommercial-ShareAlike 4.0 International License. The images or other third party material in this article are included in the article's Creative Commons license, unless indicated otherwise in the credit line; if the material is not included under the Creative Commons license, users will need to obtain permission from the license holder in order to reproduce the material. To view a copy of this license, visit <http://creativecommons.org/licenses/by-nc-sa/4.0/>